

Electronic Structure, Spectra, and Magnetic Circular Dichroism of Cyclohexa-, Cyclohepta-, and Cyclooctapyrrole

Alexander Gorski,^[a] Thomas Köhler,^[b] Daniel Seidel,^[b] Jeong Tae Lee,^[b]
Grażyna Orzanowska,^[a] Jonathan L. Sessler,^{*[b]} and Jacek Waluk^{*[a]}

Abstract: Three recently obtained expanded porphyrins represent nice examples of compounds for which the electronic and spectral properties can be predicted from symmetry considerations alone. Perimeter-model-based theoretical analysis of the electronic structure of doubly protonated cyclo[6], cyclo[7], and cyclo[8]pyrrole leads to the anticipation of qualitatively the same electronic absorption and magnetic circular dichroism patterns

for all three compounds. These predictions are fully confirmed by experiments, as well as DFT and INDO/S calculations. Due to a characteristic pattern of frontier molecular orbitals, a degenerate HOMO and a strongly split LUMO pair, the three cyclopyrroles

show comparable absorption intensity in the Q and Soret regions. Magnetic circular dichroism spectra reveal both *A* and *B* Faraday terms, of which the signs and magnitudes are in remarkably good agreement with theoretical expectations. The values of the magnetic moments of the two lowest degenerate excited states have also been obtained.

Keywords: electronic structure · magnetic properties · porphyrinoids · pyrroles

Introduction

Impressive developments in the chemistry of porphyrin-related compounds are being stimulated by the prospects of their use in a wide range of fields, including medicine, environmental protection, information technology, energy conversion and storage, and, in the most general of terms, production of new functional materials. Very promising in this respect are polypyrrolic molecules containing more than four heterocyclic rings, that is, expanded porphyrins.^[1–3] One of the more intensely studied representatives of this class, the pentapyrrolic sapphyrins, have emerged lately as versatile anion binding agents.^[4,5]

Many of possible applications of porphyrinoids rely on their interaction with light, as illustrated by such spectacular

examples as photodynamic therapy,^[6–8] solar energy conversion^[9] or optical memory storage based on holography.^[10] Obviously, a prerequisite for a successful application is the detailed understanding of the electronic structure and the excited state patterns of any given system. Equally important, albeit more challenging, is the ability to predict the spectral characteristics of a particular chromophore on the basis of structural analysis. Calculations are, of course, very helpful in this respect, but a more attractive alternative would be a model, as general as possible, which could, first, account, at least qualitatively, for the spectral features, and, second, predict the response to structural perturbations, such as substitution at a particular position. For aromatic molecules this has been attempted using a simple perimeter model.^[11–17] This approach, originally applied to understand the electronic spectra of aromatic hydrocarbons, was subsequently adapted and extended to encompass magnetic circular dichroism (MCD). The perimeter model correctly accounts for the electronic and MCD patterns in numerous compounds that can be derived from either $4N+2$ ^[11–14] or $4N$ ^[15–17] π -electron perimeters. In several cases, the theoretical predictions^[18] preceded the synthesis of the systems in question and hence necessarily antedated experimental confirmation.^[19,20]

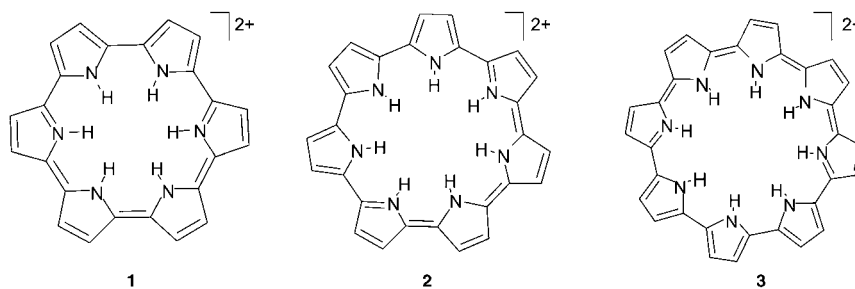
Electronic and MCD spectra of various representatives of expanded pentapyrrolic porphyrins have been recently sub-

[a] A. Gorski, G. Orzanowska, Prof. Dr. J. Waluk
Institute of Physical Chemistry
Polish Academy of Sciences, Kasprzaka 44
01-224 Warsaw (Poland)
Fax: (+48) 22-343-3333
E-mail: waluk@ichf.edu.pl

[b] Dr. T. Köhler, Dr. D. Seidel, J. T. Lee, Prof. Dr. J. L. Sessler
Department of Chemistry and Biochemistry
The University of Texas, 1 University Station A5300
Austin, TX, 78712-0165 (USA)
E-mail: sessler@mail.utexas.edu

ject to a theoretical analysis based on the perimeter model. Significant differences in the molecular orbital patterns were revealed. For instance, isosmaragdyrins were found to belong to the so-called negative-hard class of chromophores, in which the MCD pattern cannot easily be changed by structural perturbation.^[21] On the other hand, sapphyrins represent “soft” chromophores, with signs of MCD *B* terms that depend on the position of peripheral substitution.^[22]

In this work, we present experimental and theoretical results obtained for three recently synthesized expanded porphyrins, namely cyclo[6]pyrrole (**1**),^[23] cyclo[7]pyrrole (**2**),^[23] and cyclo[8]pyrrole (**3**).^[24] The doubly protonated forms of these molecules provide very rare examples of $4N+2$ π -electron chromophores in which, due to symmetry, the HOMO orbitals are degenerate, whereas the two LUMO orbitals are split. This leads to two degenerate electronic excited π - π^* states. For such a case, the perimeter model provides unambiguous predictions regarding the absorption and MCD intensities, the signs of each Faraday *A* and *B* term, and the excited state magnetic moments. Each of these predictions has been tested experimentally and, as detailed below, found to be in excellent agreement with theory for all three molecules. The electronic and spectral characteristics were also correctly reproduced by more extensive semi-empirical and DFT calculations.



of degenerate HOMO and LUMO. Two of these configurations, called sense-preserving, carry oscillator strength, but lead to small magnetic moments, $\mu^-(n,N)$. On the other hand, sense-reversing excitations are electric dipole forbidden, but have large magnetic moments, $\mu^+(n,N)$.

A crucial quantity associated with the spectral properties of a given system is the energy splitting between the two highest occupied π molecular orbitals, Δ HOMO and the analogous splitting between the lowest unoccupied pair of orbitals, Δ LUMO. Except for the special cases of 2-electron $[n]$ annulenes and $(4N+2)$ -electron $[2(N+1)]$ annulenes, both HOMO and LUMO pairs are always degenerate in the parent perimeter, but may become split as a result of perturbations that convert the ideal perimeter into the real chromophore. The diprotonated systems **1–3** can formally be derived from doubly charged $4N+2$ π electron annulenes, as shown for **1** in Figure 1. Thus, **1** is obtained from $C_{24}H_{24}^{2+}$ ($N = 5$) by a suitable distortion of the perimeter and introducing six -NH- bridges. For **2**, the precursor is $C_{28}H_{28}^{2+}$ (N

Results and Discussion

Before analyzing the experimental results, we start with theoretical predictions generated using the perimeter model. This approach describes the electronic states that originate from excitations involving the frontier π molecular orbitals of a regular n -membered, $4N+2$ electron perimeter, with pairwise degenerate orbitals, ψ_k and ψ_{-k} . In each pair of occupied orbitals, the electrons may be envisaged as circulating along the periphery in the opposite directions for ψ_k and ψ_{-k} . This creates magnetic moments that compensate for one another. The excited states are described by interactions between four singly excited HOMO–LUMO configurations involving pairs

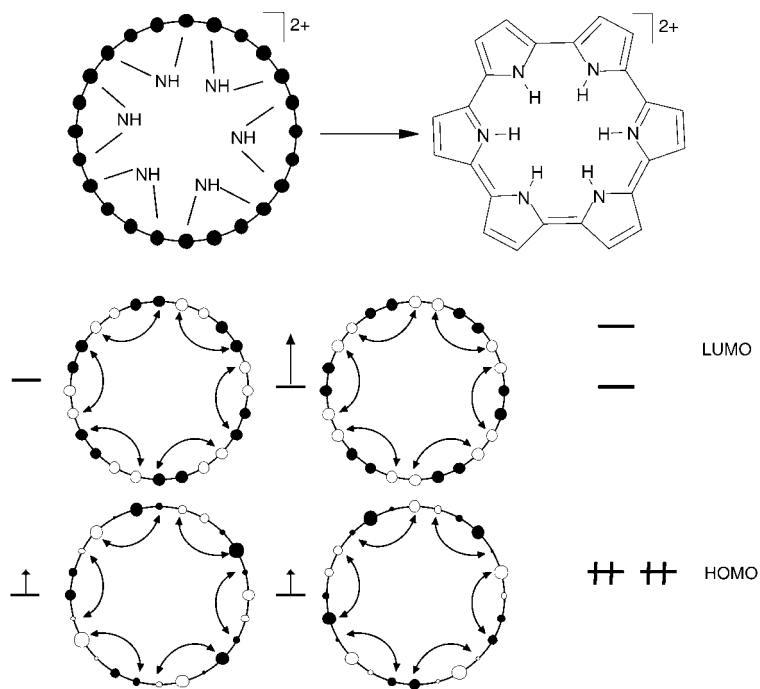


Figure 1. Top: Formal derivation of **1** from a $C_{24}H_{24}^{2+}$ perimeter; bottom: predicted energy shifts in the frontier orbitals associated with the formation of **1**.

= 6), bridged by seven -NH- groups. Finally, **3** originates from $C_{32}H_{32}^{2+}$ ($N = 7$) after adding eight -NH- linkers. These perturbations lead to the lowering of symmetry and the loss of the 24-, 28- and 32-fold rotation axis in **1-3**, respectively. However, as long as the chromophore remains planar (or all pyrrole units are tilted by the same value in the same direction), the final molecules still retain a rotation axis, albeit of lower order: C_6 for **1**, C_7 for **2**, and C_8 for **3**. In such a situation, the orbital splittings are dictated by the molecular symmetry and thus may be predicted without any calculations whatsoever.

In each of the three molecules under consideration in this study, the parent perimeter n -fold axis is converted into the corresponding (n/m) -fold axis, with $m=4$. Theoretical analysis for such a case,^[12] in which $N+1$ is an integer multiple of $n/2m$, shows that, on the basis of symmetry alone, the pair of HOMO orbitals should remain degenerate. On the other hand, the two LUMOs should split. The origin of the LUMO splitting is easy to visualize upon inspection of the form of molecular orbitals. This is illustrated for **1** in Figure 1, where the real form of the frontier orbitals is used. Bridging should have no effect for one orbital of the LUMO pair, since the NH groups are located on nodes. On the contrary, the other LUMO orbital should be strongly destabilized, since contributions from each NH bridge are additive. By contrast, the energies of both HOMO orbitals should be shifted by the same amount.

The same pattern, $\Delta\text{HOMO} = 0$ and $\Delta\text{LUMO} \neq 0$, characteristic of so-called negative-hard chromophores, is expected for **1-3**. Accordingly, all three molecules should display very similar absorption and MCD patterns. The predictions can be summarized as follows:

- two degenerate π - π^* electronic transitions, usually labeled L and B, in the order of increasing energy, should be observed in the low energy region of the electronic absorption;
- because of disparity between ΔHOMO and ΔLUMO , the L/B intensity ratio is expected to be quite high;
- since the HOMO-LUMO separation decreases from **1** to **3**, the location of L and B transitions should be shifted to the red as the size of the macrocycle increases;
- due to the degeneracy of both the L and B states, both A and B terms should be seen in the MCD spectra;
- the A terms should be negative for both L and B transitions, with the former being of larger magnitude;
- the B term should be positive for the L state and negative for the B state.

Figures 2-4 show the absorption and MCD spectra for **1-3**. The location of the absorption maxima and the values of the Faraday parameters are given in Table 1. As expected, the three molecules indeed show very similar spectral fea-

Table 1. Absorption and MCD characteristics of **1-3**.

	L transition				B transition			
	$\tilde{\nu}_0$ ^[a]	f ^[b]	A ^[c]	B ^[d]	$\tilde{\nu}_0$ ^[a]	f ^[b]	A ^[c]	B ^[d]
1	12.8	0.88	-192	67	24.9	1.38	-40	-8.2
2	10.5	0.42	-145	7.2	23.4	0.62	-29	-6.6
3	9.1	1.03	-354	20	22.6	1.43	-122	-28

[a] 10^3 cm^{-1} . [b] Oscillator strength. [c] $D^2 \mu_B$. [d] $10^{-3} D^2 \mu_B / \text{cm}^{-1}$, μ_B is the Bohr magneton.

tures. A low-lying transition is observed in the near-IR region, followed by another one, of comparable intensity, in the visible range. These transitions are located at highest energies in **1** and at lowest in **3**. An inspection of the MCD curves reveals a pattern that is roughly the derivative of the absorption, a feature that is characteristic of A terms. The A terms are negative for both L and B transitions, with their absolute values being about 3-5 times larger for the former. The B terms are positive for the L transition and negative for the B states, exactly as predicted.

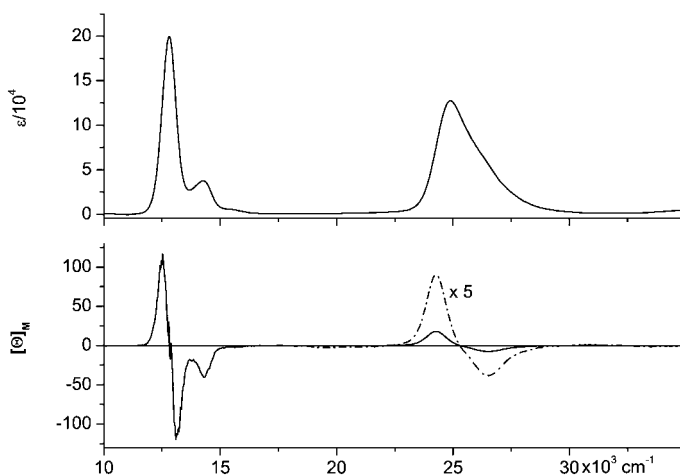


Figure 2. Electronic absorption (top) and MCD (bottom) spectra of **1** in DMSO acidified with perchloric acid.

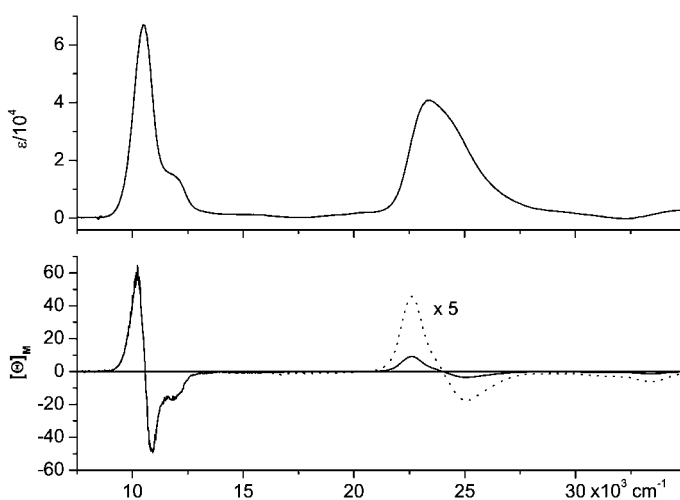


Figure 3. Electronic absorption (top) and MCD (bottom) spectra of **2** in DMSO acidified with perchloric acid.

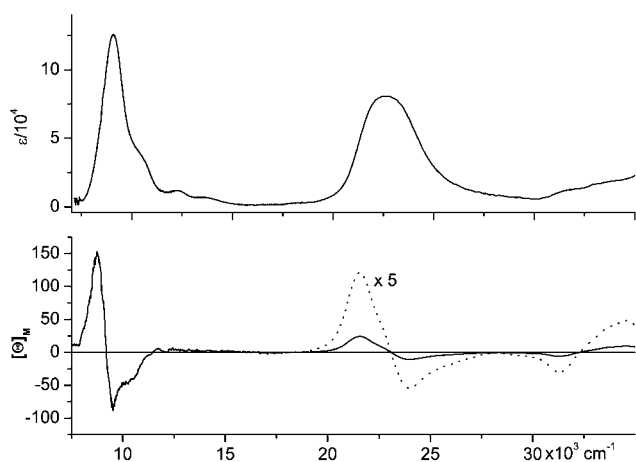


Figure 4. Electronic absorption (top) and MCD (bottom) spectra of **3** in DMSO acidified with perchloric acid.

These results can be analysed in a more quantitative fashion, by using the formulas obtained previously.^[12] The ratio of the dipole strengths, $D(L)/D(B)$ should vary as $\tan^2\beta$, where β is a measure of LUMO splitting; $\tan^2\beta = |\Delta\text{LUMO}|/(B-L)$; $B-L$ is the energy difference between the sense-preserving and sense-reversing configurations. The MCD parameters are described by the following expressions:

$$A(L)/D(L) = -\frac{1}{2}[\mu^-(n,N)\sin^2\beta - \mu^+(n,N)\cos^2\beta] \quad (1)$$

$$A(B)/D(B) = -\frac{1}{2}[\mu^-(n,N)\cos^2\beta - \mu^+(n,N)\sin^2\beta] \quad (2)$$

$$B(L)/D(L) = -(\cos^2\beta)\frac{\mu^-(n,N) + \mu^+(n,N)}{W(B) - W(L)} \quad (3)$$

$$B(B)/D(B) = (\sin^2\beta)\frac{\mu^-(n,N) + \mu^+(n,N)}{W(B) - W(L)} \quad (4)$$

where $W(B) - W(L)$ is the energy difference between these two transitions.

By using the ratio of experimentally obtained dipole strengths (Table 1), β values of 48, 51, and 53° are obtained for **1**, **2** and **3**, respectively. These values are very large, as expected, given the finding that the dipole strengths are larger for the L transitions. However, such values of β , should lead, according to Equations (1)–(2) to similar values for the A terms in L and B states, whereas the experiments shows that these values are in fact larger for the L bands. Actually, the extreme value of β predicted by the perimeter model is 45°: it corresponds to L and B transitions of equal intensity, identical A terms, and B terms with the same absolute values. We, therefore, used another approach to estimate the values of β . It is based on the experimental values of A and D combined with appropriate values of $\mu^-(n,N)$ and $\mu^+(n,N)$. The latter have been computed and tabulated

for different n and N , and for various charges present on the perimeter.^[12] Applying Equations (1) and (2) we obtain 29, 30, and 38° for the β values in **1**, **2**, and **3**, respectively. These values match quite well those estimated previously for magnesium 5,10,15,20-tetraazaporphyrin (38°), zinc tetrabenzoporphyrin (28°), and zinc phthalocyanine (38°).^[27] Also, the values of the excited state magnetic moments in the L state, $-2A/D$, 2.7, 3.5, and 3.1 μ_B for **1**, **2**, and **3**, respectively, are quite similar to those reported previously for porphyrins and phthalocyanines. For instance, values of $-3.1 \mu_B$ and $-2.3 \mu_B$ ^[28] have been estimated for octaethylporphyrin cation and anion, respectively. In metalloporphyrins, the reported values are in the range -5.4 to $-7.0 \mu_B$.^[27] One should note that the A signs in this case are opposite to those found in **1–3**, since the symmetry properties of porphyrins and phthalocyanines lead to the expectation of degenerate LUMO and nondegenerate HOMO pairs.

Simple considerations based on the molecular size could lead to the expectation that the excited state magnetic moments should be larger in **1–3** than in porphyrins and phthalocyanines, since the area encircled by the π perimeter is larger for the former. However, this is counterbalanced by the fact that in the present case of $0 = \Delta\text{HOMO} < \Delta\text{LUMO}$ the $\mu^-(n,N)$ and $\mu^+(n,N)$ contributions add up destructively [Eqs. (1)–(2)]. On the contrary, for porphyrins and phthalocyanines (positive-hard chromophores) $\Delta\text{HOMO} > \Delta\text{LUMO} = 0$. For such a case, the two contributions to the excited state magnetic moment add up constructively.^[12]

The values of the $-2A/D$ ratio for B transitions in **1–3** are lower than those for L transition, which results in smaller values of the corresponding magnetic moments: 0.68, 1.04, and 1.82 μ_B for **1**, **2**, and **3**, respectively.

Our theoretical predictions have been based so far on the assumption of regular and high symmetries, and thus either a planar geometry was assumed, or a structure in which each pyrrole unit is equally tilted out of the molecular plane in the same direction. The X-ray data show that, in the crystal, the molecules are not planar.^[23,24] In **1** and **3**, each pyrrole unit is tilted out of plane in a fashion opposite to that of its two neighbors, to give a kind of up-down-up ruffling. While the symmetry is lower in this arrangement, it still remains high, with a C_3 symmetry axis being present in **1** and a C_4 symmetry axis being present in **3**. For **2**, a pure up-down-up alternation is not possible. Indeed, the X-ray structure reveals that two adjacent pyrrole rings are tilted in the same direction.^[23] As a consequence, no high-order symmetry axis is present. The lower symmetry may be the cause of the lower values of absorption and MCD intensity values seen in **2** as compared to **1** and **3** (see Table 1).

The B3LYP/6-31G(d,p) geometry optimizations performed for nonalkylated analogues of **1–3** confirm the non-planarity, although the calculated out-of-plane deviations are smaller than those obtained from crystal structure analysis, about 6° as compared with 10° for **1** and **3** and 15° for **2**. It may be that the larger distortions seen in the crystal structure reflect hydrogen-bonding interactions involving the

counterions bound on either side of the molecular plane (either two chlorine atoms or two oxygen atoms from a sulfate group). The increased distortion seen in the case of **1–3** could also reflect the effect of steric repulsion involving the alkyl groups. In order to estimate the role of these effects, calculations were performed for additional geometries of the three chromophores. First, an “ideal”, high-symmetry planar structure was considered with C_6 , C_7 and C_8 symmetry axis present for **1–3**, respectively. For the other extreme, a strongly perturbed nonplanar structure, the X-ray geometries were used that included all the alkyl substituents. The results are compared in Table 2.

What seems crucial for the interpretation of the absorption and MCD spectral features is that the out-of-plane deviations do not alter the orbital splitting patterns predicted for high-symmetry chromophores. The calculated values of ΔHOMO and ΔLUMO reveal that the former are practically degenerate, whereas the latter are separated by large values. Somewhat surprisingly, quasi-degenerate HOMO orbitals are obtained even for **2**, the chromophore of lowest symmetry. Thus, while the nonplanar geometry may influence the absolute values of the absorptivities and Faraday terms for **1–3**, the generalized predictions from the perimeter model remain remarkably good.

Table 2 also presents the energies and oscillator strengths calculated for the four transitions stemming from the perimeter model. Both L and B states are computed as quasi-degenerate. No other electronic states are predicted near L, but several transitions, usually of low intensity, are computed in the vicinity of B. With the increased nonplanarity, more and more allowed transitions are computed close to the B states. This may accidentally result in unrealistically high values of the Faraday parameters, such as those calculated in the B region for the DFT-optimized structure of **2**. Naturally, the X-ray geometries do not lead to A terms, but the calculated pseudo-A-term patterns nicely agree with the predictions obtained for higher symmetry.

The INDO/S method yields the L transition energies closer to the experimental ones, whereas the B states are somewhat better reproduced by TD-DFT. The sums of squares of the four CI coefficients describing the excitation within four frontier orbitals are usually close to 1, indicating that the perimeter model description is a good one and that the use of this model for systems such as **1–3** is both useful and appropriate.

Summary

The application of the perimeter model to three doubly protonated cyclo[*n*]pyrroles leads to the prediction of two degenerate electronic transitions of comparable intensity. Both transitions should exhibit negative A terms, whereas the B terms should be positive for the L transition, and negative for the B transition. Gratifyingly, these predictions are all nicely confirmed by experiment. The patterns expected for a planar chromophore are not changed even when deviations from planarity are considered.

For the singly charged and neutral forms of **1–3**, the lower symmetry should result in a loss of degeneracy and a disappearance of the A terms. Four electronic transitions instead of two should be observed. In neutral chromophores, various tautomers are possible, each characterized by different spectral patterns. Current studies are aimed at assigning the absolute tautomeric structures of these species on the basis of their MCD and absorption characteristics.

Experimental and Computational Details

The synthesis and purification of **1**, **2**, and **3** have been described earlier.^[23,24] The alkylated derivatives were used, ethyl for **1** and **2** and methyl for **3** in the form of chloride (**1–2**) or sulfate (**3**) salts. The solvents included tetrahydrofuran (Merck, LiChrosol), dimethylsulfoxide (DMSO, Merck, Uvasol), methanol (Sigma-Aldrich, spectral grade) and perchloric acid (Merck, Suprapur).

Table 2. Calculated orbital splittings and electronic transition energies.

Method	$\Delta\text{HOMO}^{[a]}$	$\Delta\text{LUMO}^{[a]}$	L transition ^[b]	A term ^[c]	B term ^[d]	B transition ^[b]	A term ^[c]	B term ^[d]
1	B3LYP/6-31G(d,p) ^[e]	0.00	1.30	15.7 (0.43)	–	–	26.4 (1.74)	–
	INDO/S ^[f]	0.00	1.44	12.2 (0.09)	–246	12	27.1 (2.80)	–18
	INDO/S ^[g]	0.00	2.24	13.5 (0.26)	–475	22	30.5 (2.94)	–104
	INDO/S ^[h]	0.09	1.66	11.9 (0.09) ^[i]	–	–1642	26.9 (1.05) ^[i]	–
2	B3LYP/6-31G(d,p) ^[e]	0.02	1.32	13.9 (0.53)	–	–	24.9 (2.76)	–
	INDO/S ^[f]	0.03	1.51	10.3 (0.10)	–	19	25.6 (5.57)	–7676
	INDO/S ^[g]	0.01	1.15	10.3 (0.01)	–270	11	25.0 (3.90)	–35
	INDO/S ^[i]	0.18	2.06	10.1 (0.08) ^[i]	–	–1731	25.5 (1.08) ^[i]	–
3	B3LYP/6-31G(d,p) ^[e]	0.00	1.34	12.4 (0.66)	–	–	23.3 (3.40)	–
	INDO/S ^[f]	0.00	1.66	9.0 (0.06)	–727	30	24.2 (4.05)	–91
	INDO/S ^[g]	0.00	0.57	8.3 (0.01)	–85	5	22.9 (4.30)	–45
	INDO/S ^[k]	0.15	2.18	9.2 (0.09) ^[i]	–	–5071	23.3 (1.12) ^[i]	–
			9.3 (0.11) ^[i]	–	5114	24.5 (1.58) ^[i]	–	304

[a] eV. [b] 10^3 cm^{-1} , oscillator strength in parentheses. [c] $\text{D}^2\mu_{\text{B}}$. [d] $10^{-3} \text{ D}^2\mu_{\text{B}}/\text{cm}^{-1}$. [e] Transition energies calculated using TD-DFT. [f] Optimized B3LYP/6-31G(d,p) geometry. [g] “ideal”, high-symmetry planar geometry. [h] X-ray geometry of 2,3,6,7,10,11,14,15,18,19,22,23-dodecaethyl-cyclo[6]pyrrole. [i] Energy splitting due to loss of symmetry. [j] X-ray geometry of 2,3,6,7,10,11,14,15,18,19,22,23,26,27-tetradecaethyl-cyclo[7]pyrrole [k] X-ray geometry of 2,3,6,7,10,11,14,15,18,19,22,23,26,27,30,31-hexadecamethyl-cyclo[8]pyrrole.

Absorption spectra were measured on a Shimadzu UV 3100 spectrophotometer. MCD curves were recorded using an OLIS DSM 17 CD spectropolarimeter, equipped with a permanent magnet. The value of the magnetic field strength, 0.92 T was obtained using the MCD signal of aqueous CoSO₄ solution as a standard.^[25] Two R955 photomultipliers were used for the UV/VIS region and a pair of PbS detectors were used for wavelengths longer than 800 nm. All the measurements were carried out at 293 K.

The values of the Faraday *A* and *B* terms were obtained from the MCD spectra using the method of moments:

$$A = 33.53^{-1} \int \{[\theta](\tilde{\nu} - \tilde{\nu}_0)/\tilde{\nu}\} d\tilde{\nu}$$

$$B = -33.53^{-1} \int ([\theta]_M/\tilde{\nu}) d\tilde{\nu}$$

where $[\theta]_M$ is the magnetically induced molar ellipticity in units of deg L mol⁻¹ G⁻¹ and $\tilde{\nu}_0$ is the center of the absorption band.

Ground state geometry optimizations were performed using density functional theory (B3LYP/6-31G(d,p)) implemented in the Gaussian 03 package.^[26] Semiempirical INDO/S and DFT calculations were used for calculations of electronic transition energies; the former method also allowed the values of the Faraday terms to be computed.

Acknowledgements

This work was sponsored, in part, by grants 3T09 A 113 26 and 4T09 A 064 24 from the Polish Committee or Scientific Research. Support from the national Science Foundation (grant CHE 0107732 to J.L.S.) is also gratefully acknowledged. We thank Josef Michl and John Downing for providing us a copy of their INDO/S (DZDO) program.

- [1] J. L. Sessler, S. J. Waghorn, *Expanded, Contracted and Isomeric Porphyrins*, Elsevier, Oxford, **1997**.
- [2] J. L. Sessler, A. Gebauer, S. J. Waghorn in *Expanded porphyrins, Vol. 2* (Eds.: K. M. Kadish, K. M. Smith, R. Guilard), Academic Press, **2000**.
- [3] J. L. Sessler, D. Seidel, *Angew. Chem.* **2003**, *115*, 5292–5333; *Angew. Chem. Int. Ed.* **2003**, *42*, 5134–5175.
- [4] J. L. Sessler, J. M. Davis, *Acc. Chem. Res.* **2001**, *34*, 989–997.
- [5] J. L. Sessler, S. Camiolo, P. A. Gale, *Coord. Chem. Rev.* **2003**, *240*, 17–55.
- [6] S. B. Brown, E. A. Brown, I. Walker, *Lancet Oncol.* **2004**, *5*, 497–508.
- [7] M. R. Detty, S. L. Gibson, S. J. Wagner, *J. Med. Chem.* **2004**, *47*, 3897–3915.
- [8] T. J. Dougherty, C. J. Gomer, B. W. Henderson, G. Jori, D. Kessel, M. Korbek, J. Moan, Q. Peng, *J. Natl. Cancer Inst.* **1998**, *90*, 889–905.

- [9] D. Gust, T. A. Moore, A. L. Moore, *Acc. Chem. Res.* **2001**, *34*, 40–48.
- [10] A. Renn, U. P. Wild, A. Rebane, *J. Phys. Chem. A* **2002**, *106*, 3045–3060.
- [11] J. Michl, *Tetrahedron* **1984**, *40*, 3845–3934.
- [12] J. Michl, *J. Am. Chem. Soc.* **1978**, *100*, 6801–6811.
- [13] J. Michl, *J. Am. Chem. Soc.* **1978**, *100*, 6812–6818.
- [14] J. Michl, *J. Am. Chem. Soc.* **1978**, *100*, 6819–6827.
- [15] U. Höweler, J. W. Downing, J. Fleischhauer, J. Michl, *J. Chem. Soc. Perkin Trans. 2* **1998**, 1101–1117.
- [16] J. Fleischhauer, U. Höweler, J. Michl, *Spectrochim. Acta* **1999**, *55*, 585–606.
- [17] J. Fleischhauer, U. Höweler, J. Michl, *J. Phys. Chem. A* **2000**, *104*, 7762–7775.
- [18] J. Waluk, J. Michl, *J. Org. Chem.* **1991**, *56*, 2729–2735.
- [19] A. Gorski, E. Vogel, J. L. Sessler, J. Waluk, *J. Phys. Chem. A* **2002**, *106*, 8139–8145.
- [20] A. Gorski, E. Vogel, J. L. Sessler, J. Waluk, *Chem. Phys.* **2002**, *282*, 37–49.
- [21] A. Gorski, B. Lament, J. M. Davis, J. Sessler, J. Waluk, *J. Phys. Chem. A* **2001**, *105*, 4992–4999.
- [22] B. Lament, K. Rachlewicz, Latos-Grażyński, J. Waluk, *ChemPhys-Chem* **2002**, *3*, 849–855.
- [23] T. Köhler, D. Seidel, V. Lynch, F. O. Arp, Z. P. Ou, K. M. Kadish, J. L. Sessler, *J. Am. Chem. Soc.* **2003**, *125*, 6872–6873.
- [24] D. Seidel, V. Lynch, J. L. Sessler, *Angew. Chem.* **2002**, *114*, 2380–2383; *Angew. Chem. Int. Ed.* **2002**, *41*, 1422–1425.
- [25] B. Holmquist, *Methods Enzymol.* **1986**, *130*, 270–291.
- [26] *Gaussian 03*, Revision B.03, M. J. Frisch, G. W. Trucks, H. B. Schlegel, G. E. Scuseria, M. A. Robb, J. R. Cheeseman, J. A. Montgomery, Jr., T. Vreven, K. N. Kudin, J. C. Burant, J. M. Millam, S. S. Iyengar, J. Tomasi, V. Barone, B. Mennucci, M. Cossi, G. Scalmani, N. Rega, G. A. Petersson, H. Nakatsuji, M. Hada, M. Ehara, K. Toyota, R. Fukuda, J. Hasegawa, M. Ishida, T. Nakajima, Y. Honda, O. Kitao, H. Nakai, M. Klene, X. Li, J. E. Knox, H. P. Hratchian, J. B. Cross, C. Adamo, J. Jaramillo, R. Gomperts, R. E. Stratmann, O. Yazyev, A. J. Austin, R. Cammi, C. Pomelli, J. W. Ochterski, P. Y. Ayala, K. Morokuma, G. A. Voth, P. Salvador, J. J. Dannenberg, V. G. Zakrzewski, S. Dapprich, A. D. Daniels, M. C. Strain, O. Farkas, D. K. Malick, A. D. Rabuck, K. Raghavachari, J. B. Foresman, J. V. Ortiz, Q. Cui, A. G. Baboul, S. Clifford, J. Cioslowski, B. B. Stefanov, G. Liu, A. Liashenko, P. Piskorz, I. Komaromi, R. L. Martin, D. J. Fox, T. Keith, M. A. Al-Laham, C. Y. Peng, A. Nanayakkara, M. Challacombe, P. M. W. Gill, B. Johnson, W. Chen, M. W. Wong, C. Gonzalez, J. A. Pople, Gaussian, Inc., Pittsburgh, PA, **2003**.
- [27] A. McHugh, M. Gouterman, C. Weiss, Jr., *Theor. Chim. Acta* **1968**, *24*, 132–138.
- [28] G. Barth, R. Linder, E. Bunnenberg, C. Djerassi, *J. Chem. Soc. Perkin Trans. 2* **1974**, 696–699.

Received: December 28, 2004
Published online: April 28, 2005